IEEE Access
Multidisciplinary | Rapid Review | Open Access Journal

Received 20 May 2023, accepted 8 June 2023, date of publication 12 June 2023, date of current version 20 June 2023.

Digital Object Identifier 10.1109/ACCESS.2023.3285480

RESEARCH ARTICLE

Optimal Operation of Microgrids With Worst-Case Renewable Energy Outage: A Mixed-Integer Bi-Level Model

SAEID SHAKERINIA[1], ABBAS FATTAHI MEYABADI[2], MOJTABA VAHEDI[1], NASRIN SALEHI[3], AND MAHMOUD SAMIEI MOGHADDAM[4]

[1]Department of Electrical Engineering, Shahrood Branch, Islamic Azad University, Shahrood 1477893855, Iran
[2]Department of Electrical Engineering, Hamedan University of Technology, Hamedan 5567655888, Iran
[3]Department of Basic Sciences, Shahrood Branch, Islamic Azad University, Shahrood 1477893855, Iran
[4]Department of Electrical Engineering, Damghan Branch, Islamic Azad University, Damghan 19585-46655, Iran

Corresponding author: Abbas Fattahi Meyabadi (fattahi@hut.ac.ir)

ABSTRACT With the increasing penetration of renewable energy resources, such as wind and photovoltaic (PV) production, in future microgrids, challenges arise due to the potential interruption of these resources caused by changing weather conditions. In this paper, we propose a mixed-integer quadratic programming (MIQP) based bi-level model for the optimal operation of microgrids under worst-case (WC) scenarios of renewable energy resource outages. The upper-level problem formulates the minimization of energy loss and load shedding in a demand-side management (DSM) program, as well as optimal charging and discharging of electric vehicles (EVs) and energy storage systems (ESSs). The lower-level problem models the maximization of renewable energy curtailment to account for the worst-case realization of renewable resource outages. A decomposition and re-formulation method is adopted to solve the proposed bi-level optimization model, which includes binary variables in both levels. The proposed model and algorithm are implemented in the Julia programming language and solved with the Gurobi commercial solver. The model is analyzed using a 33-node microgrid under different cases to evaluate its performance, showcasing optimal microgrid operation results under worst-case renewable resource interruptions.

INDEX TERMS Microgrid, decomposition method, renewable resources, electric vehicles.

NOMENCLATURE

Set and Index

N	Set of microgrid nodes, indexed by n.
H	Set of hours, indexed by h.
B	Set of microgrid lines, indexed by b.
S	Set of scenarios, indexed by s.
K	Set of value of the pieces of the curve, indexed by k.

Parameters

r_b, x_b	Resistance and reactance of the line, respectively.
c_h^p, c_h^q	Cost of the real and reactive load curtailment in demand side management, respectively.
$d_{n,h}^p, d_{n,h}^q$	Initial real and reactive load, respectively.
σ_s	Probability of each scenario.
$p_{n,h,s}^r$	Power of renewable resources in each scenario.
$p_{n,h,s}^{ev}$	Charging power of electric vehicle stations in each scenario.
ρ	Power factor of DG resources.
τ	Percentage of load changes.
$\overline{f}_{b,h}^p, \overline{f}_{b,h}^q$	Maximum real and reactive power flow of the lines, respectively.
$\overline{P}_n^{DG}$	Maximum operating power of distributed generation.
$\overline{X}_n$	Maximum capacity of the battery.
$\eta_n^{ch}, \eta_n^{dis}$	Battery charging and discharging efficiency, respectively.

The associate editor coordinating the review of this manuscript and approving it for publication was N. Prabaharan.

This work is licensed under a Creative Commons Attribution-NonCommercial-NoDerivatives 4.0 License.
For more information, see https://creativecommons.org/licenses/by-nc-nd/4.0/

$\bar{p}_n^{ch}, \underline{p}_n^{ch}$	Upper and lower bound of charging power of battery, respectively.
$\bar{p}_n^{dis}, \underline{p}_n^{dis}$	Upper and lower bound of discharging power of battery, respectively.
η_n^{ev}	Battery charging efficiency of the electric vehicle.
soc_n^{min}, soc_n^{max}	Minimum and maximum battery energy in percent.
$\underline{p}_n^{ch\_ev}, \bar{p}_n^{ch\_ev}$	Minimum and maximum charging power of electric vehicles, respectively.
$\underline{p}_n^{dis\_ev}, \bar{p}_n^{dis\_ev}$	Minimum and maximum discharging power of electric vehicles, respectively.
$dr_{n,h}^{ev}$	Energy demand of electric vehicles for driving.
$\underline{e}_{n,h}^{ev}, \bar{e}_{n,h}^{ev}$	Minimum and maximum battery energy capacity in electric vehicles, respectively.
$c_{n,h}^{ev}$	Operating cost of electric vehicles.
$\beta_{n,h}^{ev}$	Slope of the k-piece for linearizing the cost curve.
$p_{n,h,k}^{ev}$	Power of the k-piece of the electric vehicles.
$\bar{p}_{h,k}^{ev}$	Maximum power considered for the kth piece in linearization.
M	Big number.
A	Outage number of renewable energy resource

Variables

$f_{b,h}^{p}, f_{b,h}^{q}$	Real and reactive power flow of lines, respectively.
$D_{n,h}^{p}, D_{n,h}^{q}$	Shifted real and reactive load, respectively.
$P_{n,h}^{r}$	Dispatched power of renewable resources.
$P_{n,h}^{ev}$	Dispatched charging power of electric vehicle stations.
$P_{n,h}^{DG}$	Real power of distributed generation (DG).
p_h^{ch}, p_h^{dis}	Charging and discharging power of the battery.
$v_{n,h}$	Microgrid node square voltage.
$e_{n,h}$	Energy level of the battery.
$e_{n,h}^{net\_ev}$	Net energy of battery charging and discharging in electric vehicles.
$p_{n,h}^{dis\_ev}, p_{n,h}^{ch\_ev}$	Discharge and charging power of the electric vehicle, respectively.
$e_{n,h}^{ev}$	State of energy in the battery of electric vehicles.

Binary Variables

$z_{n,h}$	State of charge of the battery.
$I_{n,h}^{dis\_ev}, I_{n,h}^{ch\_ev}$	State of charging and discharging of electric vehicles, respectively.
$n_{n,h}^{ev}$	State of the vehicle to the grid (V2G).
α_n	Binary variable related to the state of renewable energy resources.

I. INTRODUCTION

The primary sources of distributed renewable energy in microgrids typically consist of wind turbines and photovoltaic systems. However, these resources are vulnerable to fluctuations in weather conditions, which can result in reduced power output or complete shutdowns. As a result, any variations in the power generation from these resources or their sudden interruption can significantly impact the optimal operation of the microgrid, as determined by the daily operations of the microgrid operator.

Hence, the foremost challenge for microgrid operators is to develop an optimal operating model that accounts for potential interruptions or reductions in renewable energy resources. The motivation behind this study is to address the issue of optimal microgrid operation under worst-case scenarios, wherein renewable energy resources face outages. By incorporating such extreme conditions into the operating model, the microgrid can be made more resilient, and vulnerable points can be identified for further improvement.

A. BACKGROUND REVIEW

The authors of [1] have proposed an optimal power flow model that utilizes the method of Lagrange Multiplier to mitigate droop in AC microgrids. In [2], a model that employs the Karush-Kuhn-Tucker (KKT) optimality condition is proposed as a means to reduce operation losses in DC microgrids. In [3], a comprehensive review of various operational, planning, and control methods for DC microgrids has been conducted, encompassing different study objectives. In [4], a game theory-based approach has been proposed with the aim of maximizing the profit of microgrids in electricity markets. In [5], a proposed approach utilizes an evolutionary algorithm based on Archimedes optimization for optimizing the operation and planning of microgrids, with the objective of reducing economic costs and increasing microgrid profits. In [6], a heuristic algorithm has been proposed as a solution for optimizing the operation of microgrids, taking into account various types of distributed generation resources with the aim of minimizing economic costs. In [7], an approach based on dynamic programming has been proposed for optimizing the real-time operation of multi-energy microgrids, aiming to achieve optimal performance. In [8], a framework based on an integrated stochastic optimization model has been proposed for joint operation and maintenance in a multi-microgrid environment, with the objective of enhancing resilience. In [9], an approach based on mixed integer linear programming (MILP) has been proposed for enabling buildings to participate in enhancing microgrid resilience by leveraging synergies between microgrid and building

management systems. In [10], a generic method based on AC load flow is proposed for optimizing networks by incorporating distributed energy resources, with the objective of reducing power losses. In [11], a bi-level optimized operation strategy has been proposed with the goal of enhancing economic benefits and reducing operational risks in microgrids. In [12], a method utilizing deep Q learning has been proposed to mitigate load shedding in microgrids. In [13], a multi-stage stochastic optimization model based on mixed integer linear programming is proposed for microgrid operation under uncertainty of islanded conditions. Lastly, in [14], an energy management approach based on distributed robust model predictive control is proposed for multi-island microgrids, with the aim of mitigating the adverse effects of uncertain renewable energy output. In [15], a novel control algorithm has been developed to effectively handle the complexities associated with high levels of PV power and energy storage system integration in island microgrids. The algorithm aims to optimize the microgrid's operation, specifically targeting reduced operating costs. In [16], a comprehensive overview is provided, covering diverse topics such as optimal production planning, demand-side management, fuel and emission limitations, and the critical role of optimization in microgrid operations. In [17], a novel mixed integer linear optimization model has been introduced for the efficient energy management of large-scale energy storage systems, taking into account demand-side management strategies to maximize the total annual profit. In [18], a cutting-edge multi-objective optimization approach based on deep learning techniques has been proposed for scheduling flexible microgrids. The approach utilizes a two-stage optimization process to minimize switching and operation costs, while maximizing the overall performance. Finally, in [19], an elitist genetic algorithm has been proposed for optimal coordination of protection devices in distribution networks that incorporate distributed energy sources and microgrids. The objective is to reduce the impacts of interruptions and operational costs, ensuring robust and efficient microgrid operations. In [20], a novel mixed integer linear programming-based model has been proposed to enable effective operation of three-phase microgrids, with a specific focus on achieving optimal energy and load balance. In [21], a multi-layered approach that employs optimal power flow techniques has been presented for the operation of microgrids, with a particular emphasis on incorporating energy storage systems to enhance their performance. Additionally, in [22], a stochastic formulation based on mixed integer linear programming has been introduced as an innovative approach for the optimal operation of microgrids, taking into account the inherent uncertainties associated with wind turbines, energy storage systems, and demand response resources. These state-of-the-art methodologies offer advanced strategies for optimizing microgrid operations, addressing various challenges such as load balancing, energy storage, and uncertainty management, to improve their efficiency, resilience, and sustainability.

In [23], an innovative approach based on mixed integer nonlinear programming has been proposed for the optimal operation of multi-energy microgrids, with a specific focus on reducing operating costs while also considering environmental impacts. This approach leverages advanced optimization techniques to enable efficient and sustainable operation of microgrids. In [24], a three-level strategy has been proposed for optimal stochastic operation of microgrids, taking into account the charging of electric vehicles as a key factor. This strategy aims to enhance the resilience of microgrids by considering the uncertainties associated with electric vehicle charging patterns and incorporating them into the microgrid operation planning, thereby improving the overall performance and reliability of the microgrid system. In [25], a multi-agent-based hierarchical energy management scheme for microgrids regarding flexible power and demand response based on mixed integer linear programming (MILP) is presented. In [26], a multi-stage energy management for a hybrid microgrid with photovoltaic and hydrogen storage based on MIQP is proposed. In [27], the authors proposed a robust approach for residential microgrid energy management with renewable resources, batteries, and demand-side management. In the study [28], a control strategy based on mixed model predictive control is proposed for the energy management of grid-connected microgrids, considering battery, diesel generator, and photovoltaic systems. In [29], an internal trading strategy has been proposed for optimal energy management in the construction of microgrids with combined cooling, heating, and power systems, aiming at a multi-objective function. In [30], the authors have proposed an optimal control strategy based on the inertia of the weak grid-connected microgrid with a PV unit and energy storage system to improve the dynamic response of the microgrid. In [31], an optimal energy scheduling approach for a microgrid with electric vehicles, based on electricity market prices, is proposed to effectively manage the energy flow and charge/discharge of electric vehicles in the microgrid. In [32], an analytical optimization method is proposed for the integration of photovoltaic sources, wind turbines, and energy storage systems to improve microgrid voltage and losses. In [33], the authors have proposed a reinforcement learning (RL) approach for battery scheduling, to optimize user objectives in microgrid energy management. Table (1) has been prepared to demonstrate the superiority and differences of this study compared to recent studies.

B. RESEARCH GAP

As can be seen from the literature review and Table (1), there is a gap in studies in the analysis of the worst outage of renewable units. Most of the studies have either not considered this important or have modeled uncertainty and have not considered the complete outage of renewable resources. Considering that the outage of renewable units is modeled with a binary variable, it turns the proposed problem into a mixed integer bi-level problem, which is not the case in most microgrid studies. In this regard,

TABLE 1. Differences between this paper with recent studies.

	Upper-Level Model	Lower-Level Model	Algorithm	MO	ESS	WC	EV	DSM
This paper	MIQP	MILP	Decomposition	✓	✓	✓	✓	✓
Ref [1]	Single Level (NLP)		×	✓	×	×	×	×
Ref [2]	Single Level (MIQP)		Lyapunov	×	×	×	×	×
Ref [4]	Single Level (LP)		Game-theory	✓	✓	×	×	×
Ref [5]	Single Level (NLP)		Evolutionary	✓	✓	×	×	×
Ref [6]	Single Level (NLP)		Evolutionary	✓	×	×	×	✓
Ref [7]	LP	LP	Dynamic-programming	✓	✓	×	×	×
Ref [8]	MILP	LP	L-shaped	✓	✓	×	×	×
Ref [9]	Single Level (MILP)		Heuristic	✓	✓	×	✓	✓
Ref [10]	Single Level (NLP)		Heuristic	×	×	×	×	×
Ref [11]	MILP	NLP	Evolutionary	✓	✓	×	×	✓
Ref [12]	Single Level (NLP)		Q-Learning	×	×	×	×	×
Ref [13]	MILP	LP	Benders' decomposition	✓	✓	×	×	×
Ref [14]	LP	LP	Game theory	✓	✓	×	×	×
Ref [15]	Single Level (NLP)		Evolutionary	✓	✓	×	×	×
Ref [16]	Single Level (NLP)		Clustering	✓	×	×	×	✓
Ref [17]	Single Level (MILP)		×	✓	✓	×	×	✓
Ref [18]	Single Level (MILP)		Evolutionary	✓	✓	×	✓	×
Ref [19]	Single Level (NLP)		Evolutionary	×	✓	×	×	×
Ref [20]	Single Level (MILP)		×	×	✓	×	×	×
Ref [21]	LP	LP	Strong duality	✓	✓	×	×	×
Ref [22]	Single Level (MILP)		Monte-Carlo	✓	✓	×	×	✓
Ref [23]	Single Level (MINLP)		DICOPT	✓	✓	×	×	×
Ref [24]	LP	LP	Game theory	✓	✓	×	✓	×
Ref [25]	MILP	LP	Hierarchical	✓	✓	×	×	✓
Ref [26]	Single Level (MIQP)		×	×	✓	×	×	×
Ref [27]	MIQP	LP	Strong duality	✓	✓	✓	✓	✓
Ref [28]	Single Level (MILP)		×	×	✓	×	×	×
Ref [29]	Single Level (MILP)		Heuristic	✓	✓	×	×	×
Ref [30]	Single Level (MINLP)		×	✓	✓	×	×	×
Ref [31]	Single Level (MINLP)		Heuristic	×	✓	×	✓	✓
Ref [32]	Single Level (NLP)		Heuristic	✓	✓	×	×	✓
Ref [33]	Single Level (NLP)		Reinforcement learning	✓	✓	×	×	×

a precise algorithm to solve the proposed model should be considered.

C. RESEARCH MOTIVATION

One of the main motivations of this research is to provide an optimization model for microgrid analysis when the worst renewable energy resource outage occurs. This makes the microgrid resistant to the worst outage of renewable resources. Another major challenge of this study is the development of an algorithm to solve the proposed mixed integer bi-level model. As we know, the proposed mixed integer bi-level model cannot be converted into a single-level one by the conditions of KKT and strong duality. In this regard, an algorithm based on reformulation and decomposition has been developed to solve the challenging mixed integer bi-level model.

D. CONTRIBUTION

The main contributions of this study are as follows:

- Proposing a mixed integer bi-level optimization model based on mixed integer quadratic programming for the optimal operation of the microgrid considering the worst-case of renewable energy resource outage.
- Presenting an algorithm based on *reformulation* and *decomposition* to solve mixed-integer bi-level problems that have binary variables on both levels.
- Considering the optimal operation of distributed generation resources, demand side management, optimal charging and discharging of ESS, and optimal charging and discharging of electric vehicles in the microgrid.

E. LIMITATION OF THE EXISTING STUDIES

One of the limitations of recent studies can be pointed to the lack of modeling a mixed integer bi-level model due to the complexity of the problem and its solution. A mixed integer bi-level model cannot be solved by conventional methods such as converting to KKT conditions and strong duality because the binary variable exists in both levels; Also, algorithms for solving bi-level problems, such as Benders decomposition are not capable of solving such problems. As a result, one of the limitations of recent studies is the lack of an algorithm for solving mixed integer bi-level problems. As we know, the modeling of various problems such as the problem of the demand side management, charging and discharging of batteries, charging and discharging of electric vehicles, renewable resources, and distributed generation resources in the optimal operation of microgrids in a bi-level model increases the variables and limitations of the problem. As a result, according to Table (1), there is a limitation on the dimensions of the variables and limitations and problems considered in the optimization of microgrids in recent studies.

In the next section, the proposed bi-level model and its solution method are presented. In the third part, numerical results are analyzed and finally, conclusions and suggestions for the continuation of this study are presented.

II. THE PROPOSED METHOD

In this work, the bi-level optimization model is introduced as the primary focus, followed by a description of the decomposition-based method employed to solve the problem. The mixed integer bi-level model is divided into an upper-level problem and a lower-level problem, which are presented in detail below, outlining the formulation and objectives of each problem.

A. UPPER LEVEL PROBLEM

The upper-level problem is a mixed integer quadratic programming model for the optimal operation of the microgrid with the presence of energy storage systems, demand-side management programs, distributed generation, electric vehicles, and renewable energy resources. The multi-objective function of the upper-level problem is shown in (1a). The proposed multi-objective function in the upper-level problem includes the reduction of 5 terms, which are respectively equal to reducing the cost of energy losses, reducing active and reactive network load curtailment, reducing power curtailment of renewable resources, and finally reducing the power curtailment of electric vehicle charging stations.

$$\begin{aligned}\min \sum_{b\in B}\sum_{h\in H} H\times r_b\left(f_{b,h}^{p2}+f_{b,h}^{q2}\right)&\\ +\sum_{n\in N}\sum_{h\in H} c_h^p\left(d_{n,h}^p-D_{n,h}^p\right)&\\ +\sum_{n\in N}\sum_{h\in H} c_h^q\left(d_{n,h}^q-D_{n,h}^q\right)&\\ +\sum_{s\in S}\sigma_s\left(\sum_{n\in N}\sum_{h\in H}\left(p_{n,h,s}^r-P_{n,h}^r\right)\right.&\\ \left.+\sum_{n\in N}\sum_{h\in H}\left(p_{n,h,s}^{ev}-P_{n,h}^{ev}\right)\right)&\end{aligned} \tag{1a}$$

Equations (1b) and (1c) demonstrate the balance of active and reactive power in the microgrid, respectively.

$$\begin{aligned}\sum_{nm\in N} f_{nm,h}^p-\sum_{mn\in N} f_{mn,h}^p+p_{n,h}^{dis}+P_{n,h}^r+P_{n,h}^{DG}-D_{n,h}^p&\\ -P_{n,h}^{ev}-p_{n,h}^{ch}=0&\end{aligned} \tag{1b}$$

$$\sum_{nm\in N} f_{nm,h}^q-\sum_{mn\in N} f_{mn,h}^q+\rho P_{n,h}^r+\rho P_{n,h}^{DG}-D_{n,h}^q=0 \tag{1c}$$

Equations (1d) and (1e) indicate the limit of the total active and reactive loads changed in the microgrid, respectively. Constraints (1f) and (1g) indicate the range of changes in active and reactive loads, respectively.

$$\sum_{n\in N} d_{n,h}^p=\sum_{n\in N} D_{n,h}^p\ \forall h\in H \tag{1d}$$

$$\sum_{n\in N} d_{n,h}^q=\sum_{n\in N} D_{n,h}^q\ \forall h\in H \tag{1e}$$

$$d_{n,h}^p-d_{n,h}^p\tau\le D_{n,h}^p\le d_{n,h}^p+d_{n,h}^p\tau\ \forall h\in H, n\in N \tag{1f}$$

$$d_{n,h}^q-d_{n,h}^q\tau\le D_{n,h}^q\le d_{n,h}^q+d_{n,h}^q\tau\ \forall h\in H, n\in N \tag{1g}$$

The limits of the real and reactive power flow of the lines are demonstrated by (1h) and (1i), respectively.

$$-\overline{f}_{b,h}^p\le f_{b,h}^p\le\overline{f}_{b,h}^p\ \ \forall h\in H, n\in N \tag{1h}$$

$$-\overline{f}_{b,h}^q\le f_{b,h}^q\le\overline{f}_{b,h}^q\ \ \forall h\in H, n\in N \tag{1i}$$

The constraint of microgrid node voltage is shown by (1j).

$$0.9^2\le v_{n,h}\le 1.1^2\ \ \forall h\in H, n\in N \tag{1j}$$

The square node voltage of the microgrid is obtained according to equation (1k).

$$v_{n,h}=v_{m,h}-2\left(r_b f_{b,h}^p+x_b f_{b,h}^q\right)\forall h\in H, n\in N \tag{1k}$$

The operating limit of distributed generation is demonstrated by (1l).

$$\underline{P}_n^{DG}\le P_{n,h}^{DG}\le\overline{P}_n^{DG}\forall h\in H, n\in N \tag{1l}$$

The charging and discharging limits of ESSs are demonstrated in relations (1m) and (1n), respectively. The state of energy in the battery is shown in relation (1o). Equation (1p) demonstrates the limitation of the energy capacity of the ESS.

$$\underline{p}_n^{ch}z_{n,h}\le p_{n,h}^{ch}\le\bar{p}_n^{ch}z_{n,h}\forall h\in H, n\in N \tag{1m}$$

$$\underline{p}_n^{dis}\left(1-z_{n,h}\right)\le p_{n,h}^{dis}\le\bar{p}_n^{dis}\left(1-z_{n,h}\right)\forall h\in H, n\in N \tag{1n}$$

$$e_{n,h}=e_{n,h-1}+p_{n,h}^{ch}\eta_n^{ch}-p_{n,h}^{dis}\Big/\eta_n^{dis}\ \forall h\in H, n\in N \tag{1o}$$

$$soc_n^{min}\overline{X}_n\le e_{n,h}\le soc_n^{max}\overline{X}_n\ \forall h\in H, n\in N \tag{1p}$$

Equation (1q) demonstrates the charging limit of electric vehicle charging stations.

$$0\le P_{n,h}^{ev}\le P_{n,h,s}^{ev}\ \ \forall h\in H, n\in N, s\in S \tag{1q}$$

Equations (1r) to (1bc) demonstrate the modeling of electric vehicles in the microgrid. The net energy of battery charging and discharging in electric vehicles according to the efficiency of each battery is demonstrated in (1r). Equation (1s) indicates the rate of injected and received power from or to the microgrid by electric vehicles, which is computed by the charging and discharging amount of the battery. The state of charging and discharging of electric vehicles is illustrated in (1t). Relations (1u) and (1v) demonstrate the limitation of charging and discharging power of electric vehicles, respectively. Equation (1w) indicates the state of energy in the battery of electric vehicles. Equation (1x) conducts the limitation of battery energy capacity in electric vehicles. Relations (1y) and (1z) consider the net energy of electric vehicle battery charging and

discharging and the available energy of the electric vehicle battery in the first and last hours. Equations (1bb) to (1bd) illustrate the charging and discharging cost curves of electric vehicle batteries.

$$e^{net\_ev}_{n,h} = p^{dis\_ev}_{n,h} - \eta^{ev}_{n} p^{ch\_ev}_{n,h} \tag{1r}$$

$$P^{ev}_{n,h} = p^{dis\_ev}_{n,h} - p^{ch\_ev}_{n,h} \tag{1s}$$

$$I^{dis\_ev}_{n,h} + I^{ch\_ev}_{n,h} = n^{ev}_{n,h} \tag{1t}$$

$$I^{ch\_ev}_{n,h} \underline{p}^{ch\_ev}_{n} \le p^{ch_{ev}}_{n,h} \le I^{ch_{ev}}_{n,h} \overline{p}^{ch\_ev}_{n} \tag{1u}$$

$$I^{dis\_ev}_{n,h} \underline{p}^{dis\_ev}_{n} \le p^{dis_{ev}}_{n,h} \le I^{dis_{ev}}_{n,h} \overline{p}^{dis\_ev}_{n} \tag{1v}$$

$$e^{ev}_{n,h} = e^{ev}_{n,h-1} - e^{net_{ev}}_{n,h} - \left(1 - n^{ev}_{n,h}\right) dr^{ev}_{n,h} \tag{1w}$$

$$\underline{e}^{ev}_{n,h} \le e^{ev}_{n,h} \le \overline{e}^{ev}_{n,h} \tag{1x}$$

$$e^{ev}_{n,h=1} = e^{ev}_{n,h=24} \tag{1y}$$

$$e^{net\_ev}_{n,h=1} = e^{net\_ev}_{n,h=24} \tag{1z}$$

$$c^{ev}_{n,h} = n^{ev}_{n,h} \sum_{k=1}^{K} \beta^{ev}_{n,k} p^{ev}_{n,h,k} \tag{1bb}$$

$$n^{ev}_{n,h}\left(e^{ev}_{n,h} - e^{ev}_{n,h-1}\right) \ge -\sum_{k=1}^{K} p^{ev}_{n,h,k}, n^{ev}_{n,h}$$

$$\left(e^{ev}_{n,h} - e^{ev}_{n,h-1}\right) \le \sum_{k=1}^{K} p^{ev}_{n,h,k} \tag{1bc}$$

$$0 \le p^{ev}_{n,h,k} \le \overline{p}^{ev}_{h,k} \tag{1bd}$$

As can be seen, equations (1bb) and (1bc) are non-linear. To linearize these two equations, we use the big M-method. By defining a new variable and a large parameter M, we add new constraints to the model. For this purpose, the linear model of equation (1bb) is as follows. Note that $\Omega_{t,n}$ illustrates the product of two expressions $n^{ev}_{n,h}$ and $\sum_{k=1}^{K} \beta^{ev}_{n,k} p^{ev}_{n,h,k}$.

$$c^{ev}_{n,h} = \Omega_{n,h} \tag{1be}$$

$$\Omega_{n,h} \le M \times n^{ev}_{n,h}$$

$$\Omega_{n,h} \le \sum_{k=1}^{K} \beta^{ev}_{n,k} p^{ev}_{n,h,k} \tag{1bg}$$

$$\Omega_{n,h} \ge \sum_{k=1}^{K} \beta^{ev}_{n,k} p^{ev}_{n,h,k} - \left(1 - n^{ev}_{n,h}\right) \times M \tag{1bh}$$

$$\Omega_{n,h} \ge 0 \tag{1bi}$$

As can be seen, equations (1be) to (1bi) are completely linear and replace equation (1bb). In the same way and with the same method, equation (1bc) can be linearized, by defining a new variable and a big number. In such a way that $\Psi_{n,h}$ is equal to the new variable to define the multiplication of two terms $(e^{ev}_{n,h} - e^{ev}_{n,h-1})$ and $n^{ev}_{n,h}$.

$$\Psi_{n,h} \ge -\sum_{k=1}^{K} p^{ev}_{n,h,k} \tag{1bj}$$

$$\Psi_{n,h} \le \sum_{k=1}^{K} p^{ev}_{n,h,k} \tag{1bk}$$

$$\Psi_{n,h} \le n^{ev}_{n,h} \times M \tag{1bl}$$

$$\Psi_{n,h} \le \left(e^{ev}_{n,h} - e^{ev}_{n,h-1}\right) \tag{1bm}$$

$$\Psi_{n,h} \ge \left(e^{ev}_{n,h} - e^{ev}_{n,h-1}\right) - \left(1 - n^{ev}_{n,h}\right) \times M \tag{1bn}$$

$$\Psi_{n,h} \ge 0 \tag{1bo}$$

As presented, equations (1a) to (1bo) are the upper-level problem. The common variable between the upper-level problem and the lower-level problem is the power of renewable energy resources ($P^{r}_{n,h}$).

B. LOWER LEVEL PROBLEM

In the lower-level problem, the maximization of renewable energy sources is done. By modeling the lower-level problem, the grid is operated with worst-case renewable energy resource outages. The objective function of the lower-level problem is shown in (2a). As can be seen, the increase in the power outage of renewable energy resources is considered a lower-level problem.

$$\max \sum_{n\in N} \sum_{h\in H} \sum_{s\in S} p^{r}_{n,h,s} - P^{r}_{n,h} \tag{2a}$$

The limitation of operating renewable energy resources is illustrated in (2b). Here α_n demonstrates the binary variable related to the state of renewable energy resources. If α_n is equal to 1, renewable energy is active, otherwise, it is disconnected from the microgrid. A demonstrates the outage number of renewable energy resource units considered. In this paper, the number of different outages is also considered which is analyzed in the results section. It can be seen that the lower-level model is in the form of relations (2a) to (2c).

$$0 \le P^{r}_{n,h} \le p^{r}_{n,h,s} \alpha_n \forall h \in H, n \in N, s \in S, \alpha_n \in \{0, 1\} \tag{2b}$$

$$\sum_{n\in N} \alpha_n = A \tag{2c}$$

Finally, the proposed bi-level optimization model is in the form of relations (1) to (2). The method of solving the proposed bi-level model is described in the next section.

C. PROPOSED SOLUTION METHOD

The proposed bi-level optimization problem is in the general form of equations (3a) to (3d), that relation (3a) is the objective function of the upper-level problem and (3b) its constraints, and relation (3c) is the objective function of the lower level and (3d) the constraints related to it.

$$\min \sum_{b\in B} \sum_{h\in H} H \times r_b \left(f^{p2}_{b,h} + f^{q2}_{b,h}\right) \tag{3a}$$
$$+ \sum_{n\in N} \sum_{h\in H} c^{p}_{h} \left(d^{p}_{n,h} - D^{p}_{n,h}\right)$$
$$+ \sum_{n\in N} \sum_{h\in H} c^{q}_{h} \left(d^{q}_{n,h} - D^{q}_{n,h}\right)$$

$$+\sum_{s\in S}\sigma_s\left(\sum_{n\in N}\sum_{h\in H}\left(p^r_{n,h,s}-P^r_{n,h}\right)\right.$$
$$\left.+\sum_{n\in N}\sum_{h\in H}\left(p^{ev}_{n,h,s}-P^{ev}_{n,h}\right)\right)$$
$$s.t.\ (1b)-(1bo) \tag{3b}$$
$$\max\sum_{n\in N}\sum_{h\in H}\sum_{s\in S}p^r_{n,h,s}-P^r_{n,h} \tag{3c}$$
$$s.t.\ (2b)-(2c) \tag{3d}$$

As seen, the bi-level model (3) has a binary composite structure in both levels, which we act as follows to solve it, which is obtained from [34].

We subsequently utilize the *reformulation-and-decomposition* scheme which executes the *column-and-constraint* generation plot to calculate (4) by a master problem and two subproblems. To demonstrate the steps of the proposed computational methodology, we first write the brief form (4) as follows.

$$\min ax+by \tag{4a}$$
$$s.t.\ By+Cr_n=d \tag{4b}$$
$$Ax+Dy\geq l, x\epsilon\{0,1\} \tag{4c}$$
$$\|Hy\|\leq hy \tag{4d}$$
$$where\ r_n\in \text{argmax}\{e_n(r_n+y_n):\ \tag{4e}$$
$$s.t.\ G_nw_n+E_nr_n+O_ny_n=f_n \tag{4f}$$
$$F_nw_n+K_nr_n\leq k_n \tag{4g}$$
$$r_n\geq 0, w_n\in\{0,1\}\}\forall n\in N \tag{4h}$$

where x and y indicate the upper level binary and continuous variables, and r_n and w_n display the lower-level continuous and binary variables.

The coefficient matrices and vectors $(A, a, B, b, E_n, e_n, l, D, d, F_n, f_n, G_n, H, h, K_n, k_n, O_n)$ with suitable dimensions are regarding these variables. In inequality (4d), we let symbol $\|\bullet\|$ show the l_2-norm for matrices (vectors). Equation (4e) indicates the objective function and (4f)-(4h) are the lower level's primal constraints model.

For algorithm development, we need to build a decomposable structure; we have used [34] to reformulate the bi-level model (4), so duplicating the lower-level variables and constraints in the upper-level model and adding an extra limitation (5e) as follows:

$$\min ax+by \tag{5a}$$
$$s.t.\ [(4b)-(4d)] \tag{5b}$$
$$G_nw'_n+E_nr'_n+O_ny_n=f_n, F_nw'_n+K_nr'_n\leq k_n \tag{5c}$$
$$r'_n\geq 0, w'_n\in\{0,1\} \tag{5d}$$
$$e_n\left(r'_n+y_n\right)$$
$$\leq\max\{e_n(r_n+y_n):\ \tag{5e}$$
$$s.t.\ G_nw_n+E_nr_n+O_ny_n=f_n, F_nw_n+K_nr_n\leq k_n \tag{5f}$$
$$r_n\geq 0, w_n\in\{0,1\}\}\forall n\in N \tag{5g}$$

where the repeated lower-level variables in the upper-level are denoted by r'_n and w'_n. Notice that (5c)-(5d) are specified for the worst-case realization of renewable resource outages. Due to (5e), we derive that model (5a)-(5g) is equipollent to the main optimization of the bi-level (3). Eventhough more complex than (3), the reformulated problem (5a)-(5g) propose a helpful outline to conclude non-trivial bounds to problem (3). Let $\mathcal{W}$ be the set of all feasible realization of w_n and $\tilde{w}_n$ be a characteristic realization of w_n. By enumeration w_n and presentation its continuous variables $\hat{r}^n_n$, we can rewrite (5e)-(5g) as follows:

$$e_n\left(r'_n+y_n\right)$$
$$\leq\max\left\{e_n\left(\hat{r}^{\tilde{w}_n}_n+y_n\right)\right. \tag{6a}$$
$$s.t.\ G_n\hat{r}^{\tilde{w}_n}_n+E_n\tilde{w}_n+O_ny_n=f_n \tag{6b}$$
$$K_n\hat{r}^{\tilde{w}_n}_n+F_n\tilde{w}_n\leq k_n \tag{6c}$$
$$\hat{r}^{\tilde{w}_n}_n\geq 0, \tilde{w}_n\in\mathcal{W},\ n\in N \tag{6d}$$

When $\tilde{w}_n$ is given, it is observed that, the right-hand side of (6a)-(6d) are a linear model. Moreover rather than having a complete enumeration, (6a)-(6d) developed pursuant to a subset $\tilde{\mathcal{W}}\subseteq\mathcal{W}$ results in a relaxation of (5a)-(5g), or equality the main bi-level problem (3). As explained in the next part, these aspects enable us to develop the decomposition method using the *column-and-constraint* generation method [35].

1) SUBPROBLEM

The following subproblem SP1_n is formulated and calculated for the worst-case renewable energy outage, for a given upper-level decision (x^*, y^*):

$$\mathbf{SP1_n}:\Psi_n\left(x^*,y^*_n\right)$$
$$=\max e_n\left(r_n+y^*_n\right) \tag{7a}$$
$$s.t.\ G_nw_n+E_nr_n+O_ny^*_n=f_n:\lambda_n \tag{7b}$$
$$F_nw_n+K_nr_n\leq k_n:\mu_n \tag{7c}$$
$$r_n\geq 0, w_n\in\mathcal{W} \tag{7d}$$

Eventhough the problem SP1_n is a mixed-integer linear, for a fixed w_n, the rest of the problem is linear. The dual variables of constraints (7b) and (7c) are denoted by λ_n and μ_n. Specifically, SP1_nproposes an optimal solution of lower-level (3c)-(3d) for the investment plan (x^*, y^*_n). However, it could have several solutions. The second subproblem, i.e., SP2, derives from one that is regarding the upper-level problem. So SP2 is mixed-integer model, as follows:

$$\mathbf{SP2}:\Psi\left(x^*,y^*\right)$$
$$=\min ax+by \tag{8a}$$
$$s.t.\ [(7b)-(7d)] \tag{8b}$$
$$e_n(r_n+y_n)\leq\Psi_n\left(x^*,y^*_n\right)\forall n\in N \tag{8c}$$

2) MASTER PROBLEM

With the formulations (5)-(6), the master problem is created by: 1) duplicating the lower-level variables (show by

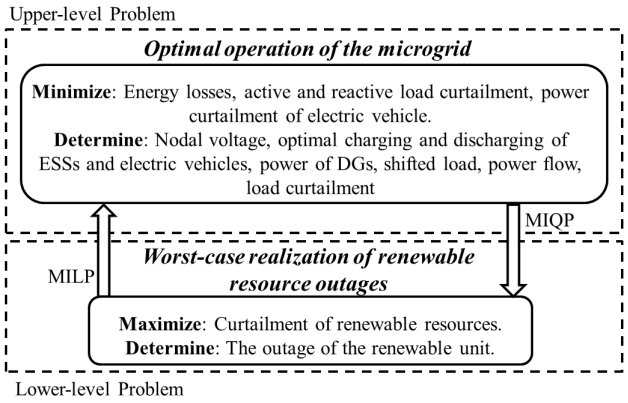

FIGURE 1. Framework of the proposed approach.

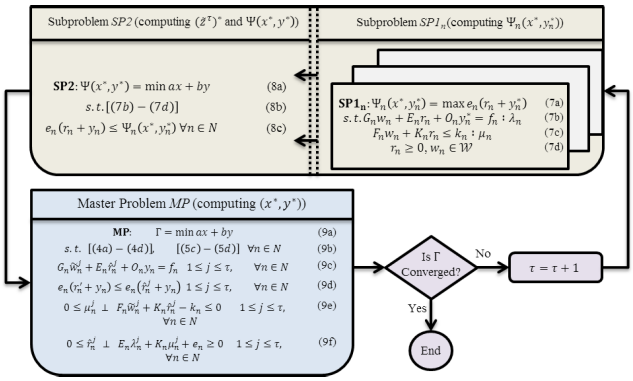

FIGURE 2. Flowchart of the proposed decomposition algorithm.

w_n' *and* r_n') and constraints in the upper-level model; and 2) replacing the lower-level model (in iteration n) of a fixed realization $\tilde{w}_n^j \in \tilde{\mathcal{W}} \subseteq \mathcal{W}$ by its *Karush–Kuhn–Tucker* conditions (continuous primal variables are marked by $\hat{r}_n^j$, and dual variables by λ_n^j and μ_n^j). The master problem's dense form is suggested within the algorithm description (see (9) below and also [35]). In the following, the steps of the modified *column-and-constraint* generation decomposition method are given to solve the whole bi-level optimization model. Let LB and UB be the lower and upper bounds,ϵ be the optimality tolerance and τ be the repetition index.

This method dynamically provides more strong lower bounds (from the master problem) and upper bounds (from subproblems) and, in each iteration, it adds new variables and constraints to the master problem until the difference between bounds is not bigger than optimal tolerance ϵ. The mathematical proof of the limited convergence of this algorithm to the optimal value can be found in [34] and [35]. Fig. 1 demonstrates the framework of the presented approach. Fig. 2 demonstrates the flowchart of the proposed bi-level solution. It should be noted to confirm that the master problem is a complementary program that can be transformed into a regular mixed-integer quadratic program by linearizing (9e)-(9f) using the big-M method. Accordingly, existing commercial mixed-integer solvers can be used to compute all subproblems and master problem.

The results of data analysis considering different study cases are presented in the next part of the paper.

III. NUMERICAL RESULTS

In this paper, the microgrid of 33 nodes is considered for the analysis of the proposed method and model. The proposed microgrid has 33 buses and 32 lines, and distributed generation resources are installed in nodes 6, 13, 16, 18, 22, 30, and 33. The energy storage system and PV resources are installed in nodes 3, 6, 10, 14, 21, 26, 30, and 32, respectively. As well as wind generation are located in nodes 6, 12, 17, 20, 27, and 33, respectively. Charging stations for electric vehicles are located on nodes 8, 17, and 28, respectively.

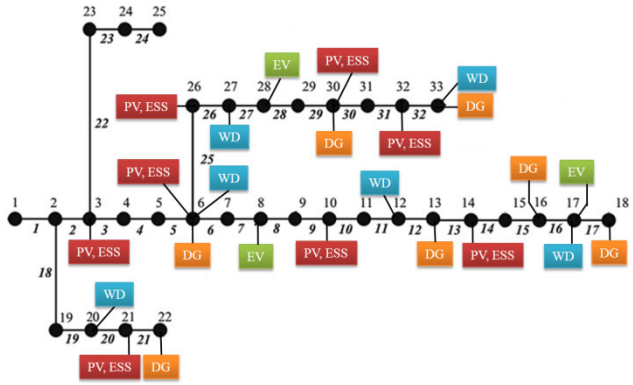

FIGURE 3. Proposed 33-node microgrid.

TABLE 2. Data of batteries and DGs.

Parameters	Value
$\eta_n^{ch}, \eta_n^{dis}$	0.95
$\overline{p}_n^{ch}, \overline{p}_n^{dis}$ (kW)	100
$\underline{p}_n^{ch}, \underline{p}_n^{dis}$ (kW)	0
$\overline{X}_n$ (kWh)	500
soc_n^{min}, soc_n^{max} (%)	10, 90
$e_{n,1}$	20
$\overline{P}_n^{DG}$ (kW)	1000
$\underline{P}_n^{DG}$ (kW)	0
Ramp rate (kW)	200
ρ	0.85

Figure (3) illustrates the schematic of the proposed microgrid. The location of each of the wind renewable energy sources, electric vehicles, and energy storage systems along with photovoltaic sources is shown in this figure.

Table (2) illustrates the data related to the battery and distributed generation resources. Lithium-type energy storage systems with 95% efficiency are considered. The maximum charge and discharge power is 100 kW and the maximum battery capacity is 500 kWh. The initial energy of the battery in the first hour is considered equal to 20 kW. The minimum and maximum SOC of the battery is considered to be 10 and 90%. The maximum power of distributed generation resources is 1000 kW and the power factor is 0.85. The maximum capacity of wind and photovoltaic renewable sources for each unit is considered to be 500 kW.

TABLE 3. Comparison of the results obtained from different cases in the 33-bus network.

	Case 1	Case 2	Case 3	Case 4
Energy Losses (MWh)	0.166	0.172	0.181	0.197
Min voltage (p.u)	0.9749	0.9740	0.9734	0.970
Load shedding (MWh)	0	0	0	0
PV outage (node)	-	14 21	10 14 21 32	6 10 14 21 26 32
Wind outage (node)	-	12 27	12 17 27 33	6 12 17 20 27 33
Total production of DGs (MWh)	47.5	48.9	51	53
Total production of PVs (MWh)	2.62	2.05	1.5	0.88
Total production of winds (MWh)	3.6	2.78	1.6	0
CPU time (s)	8	11	12	12

To analyze the proposed model and show the impact of the number of worst-case renewable resource outages, the following cases are considered.

Case 1: Without the outage of renewable energy resources.

Case 2: The outage of two PV renewable energy units and two wind units.

Case 3: The outage of four PV renewable energy units and four wind units.

Case 4: The outage of six PV renewable energy units and six wind units

Table (3) demonstrates the results of simulations in different considered cases. Briefly, it can be seen that the proposed model has been resistant to any number of worst cases of renewable resource outage so that no load shedding has occurred in any of the study cases. According to the results of table (3), the impact of the worst-case scenario of renewable resources outage is on the energy losses and voltage of the nodes. It can be concluded that the optimal operation of the microgrid in the upper-level problem has caused no load curtailment with optimal management between load and energy.

In the first case, where there is no curtailment of renewable energy resources, the energy loss is equal to 0.166 MWh and the lowest network voltage is equal to 0.9749 p.u. The maximum production of distributed generation, PV, and wind energy are 47.5, 2.62, and 3.6 MWh respectively for 24 hours. In the second case, two PV and wind renewable resource units are disconnected from the microgrid. As can be seen, based on the proposed model, the worst-case of renewable resources outage in this case for PV is equal to nodes 14 and 21 and for wind energy is equal to nodes 12 and 27. The energy loss, in this case, is equal to 0.172 MWh and the lowest network voltage is equal to 0.9740 p.u. The maximum production of distributed generation, PV, and wind energy are 48.9, 2.05, and 2.78 MWh respectively for 24 hours. In the third case, four PV and wind renewable resource units are disconnected from the microgrid. As can be seen, based on the proposed model, the worst-case of renewable resources outage in this case for PV is equal to nodes 10, 14, 21, and 32 and for wind energy is equal to nodes 12, 17, 27, and 33. The energy loss, in this case, is equal to 0.181 MWh and the lowest network voltage is equal to 0.9734 p.u. The maximum production of distributed generation, PV, and wind energy are 51, 1.5, and 1.6 MWh respectively for 24 hours. In the fourth case, six PV and wind renewable resource units are disconnected from the microgrid. As can be seen, based on the proposed model, the worst-case of renewable resources outage in this case for PV is equal to nodes 6, 10, 14, 21, 26, and 32 and for wind energy is equal to nodes 6, 12, 17, 20, 27, and 33. The energy loss, in this case, is equal to 0.197 MWh and the lowest network voltage is equal to 0.97 p.u. The maximum production of distributed generation, PV, and wind energy are 53, 088, and 0 MWh respectively for 24 hours.

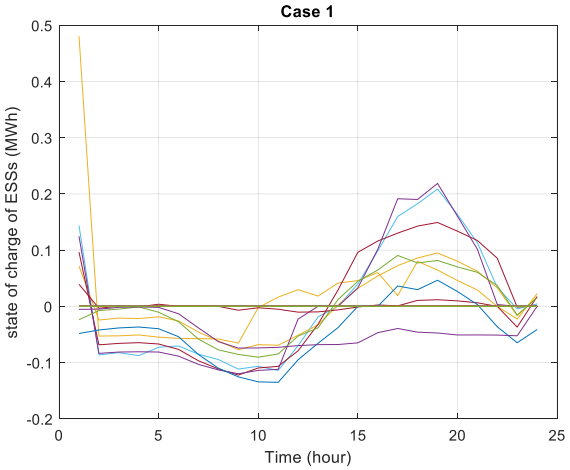

FIGURE 4. Optimal charging and discharging of energy storage systems in the first case.

Finally, the simulation results showed that according to the worst outage of renewable energy resources, the microgrid with the proposed model has high flexibility and no load curtailment occurred in any number of outages of renewable energy resources. The results prove that the proposed model and method can be effective in the operation of microgrids with the possibility of the worst outage of renewable energy resources.

Figure (4) demonstrates the optimal charging and discharging of batteries. The vertical negative axis indicates the charge and the vertical positive axis indicates the discharge of the batteries. As it seems, most batteries are charged in the early hours when energy is cheap and discharged during peak hours. It can be seen that all the batteries in the microgrid have the same behavior, only their charging and discharging power are different. In this figure, each color belongs to an energy storage system in nodes 3, 6, 10, 14, 18, 21, 26, 30 and 32.

Figure (5) demonstrates the production of DG units. It can be seen that most of the DG units have production during

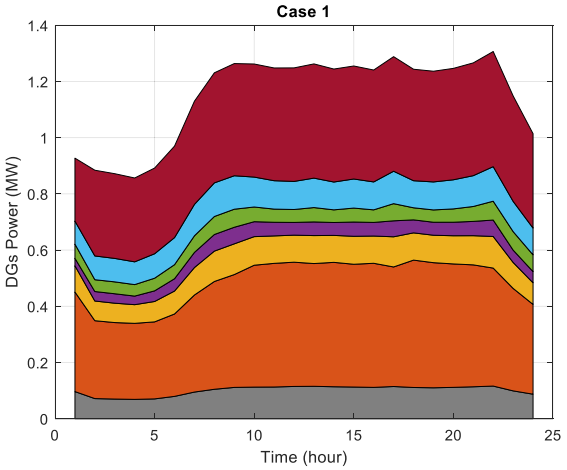

FIGURE 5. Production of DG units in the first case.

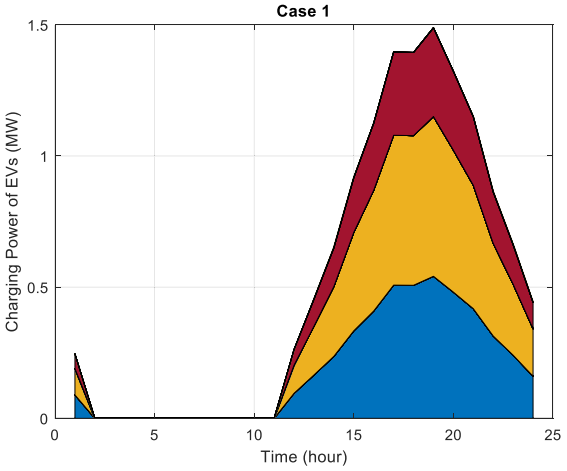

FIGURE 6. Charging electric vehicles in the first case.

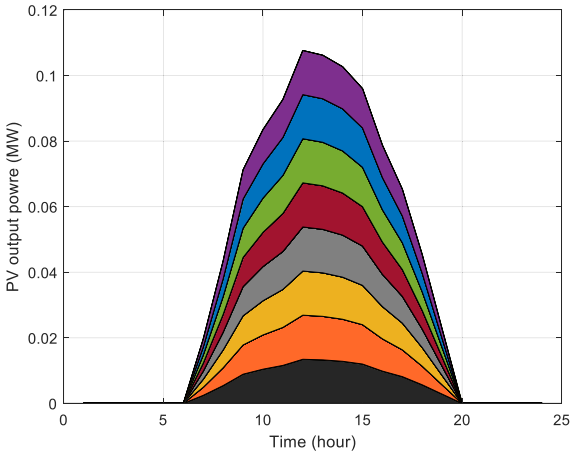

FIGURE 7. PV generation in the first case.

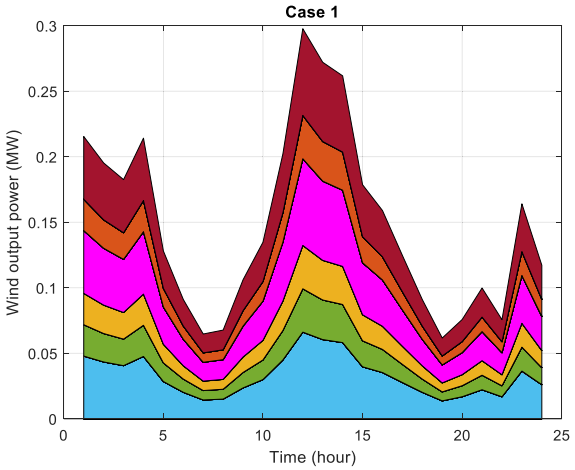

FIGURE 8. Wind generation in the first case.

peak times. In this figure, red, blue, green, purple, yellow, orange, and gray colors indicate distributed generation power in nodes 33, 30, 22, 18, 16, 13, and 6, respectively.

Figure (6) illustrates the charging of electric vehicles during the day in the first case. It indicates the energy purchased during the day in the first case. It can be seen that most energy purchases are related to peak load times. In this figure, the colors red, yellow, and blue demonstrate the charging power of electric vehicles at nodes 17, 28, and 8, respectively.

Figures (7) and (8) demonstrate the production of PV and wind units during the day, respectively. In these figures, the production of each PV or wind unit is shown with a different color. As you can see, PV units only produce from 6:00 AM to 7:00 PM. In the same way, the highest production in wind units is from 11 am to 2 pm and the lowest amount of production is from 6 am to 10 am and 7 pm to 10 pm. It should be noted that this amount of production for PV and wind units is based on the worst-case scenario of the production of PV and wind resources. In Figure (7), purple, blue, green, red, gray, yellow, orange and black are the power of PV resources in nodes 3, 6, 10, 14, 18, 21, 26, 30, and 32, respectively. In Figure (8), blue, green, yellow, pink, orange, and red colors correspond to the power of wind units at nodes 6, 12, 17, 20, 27, and 33, respectively.

Figure (9) illustrates a comparison between the initial network loads and the changed loads in the demand-side management program. As can be seen, the peak load has been reduced in the demand side management program. Here, the blue curve illustrates the changed load in the demand-side management program, and the orange curve is the initial microgrid load (unchanged). This figure demonstrates the exact performance of the demand side management in reducing the microgrid peak.

Finally, Figure (10) demonstrates the voltage of distribution network buses every hour. It can be seen that most of the voltage changes are in the range (0.996 to 1 p.u). This illustrates that in the proposed model, the voltage of the distribution network is well maintained within the allowed range.

To illustrate the impact of battery energy storage systems (BESS) on important microgrid indicators such as loss and voltage, Table 4 has been prepared. Here, the case where the battery is in the microgrid is also compared with the case where the battery is not in the microgrid. As can be seen, energy losses without batteries have increased by about 79%,

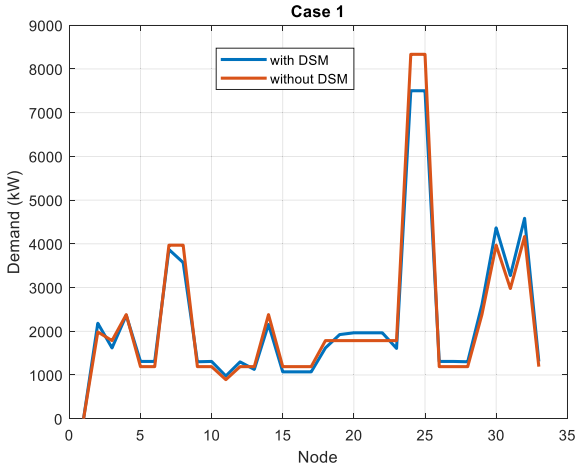

FIGURE 9. Comparison between the initial network loads and the modified loads in the first case.

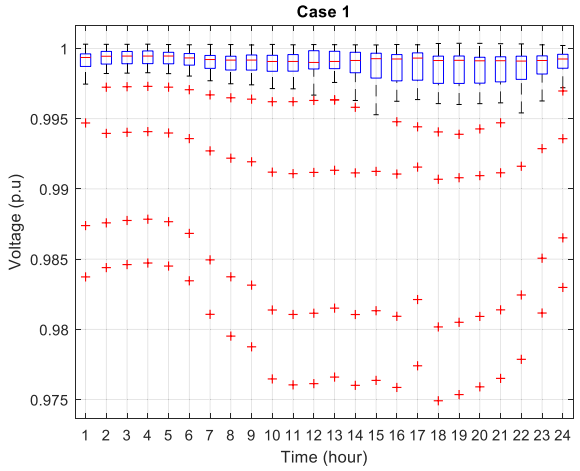

FIGURE 10. Box plot of changes in the size of the distribution network bus voltage during the day in the first case.

TABLE 4. The effect of battery in the optimization of microgrids.

	With BESS	Without BESS
Energy Losses (MWh)	0.166	0.298
Min voltage (p.u)	0.9749	0.9710

this demonstrates the high impact of energy storage systems in reducing microgrid energy losses. On the other hand, it can be seen that the battery had an almost half percent effect on improving the microgrid voltage.

IV. CONCLUSION

In this paper, a bi-level model based on mixed-integer quadratic programming (MIQP) was proposed for the optimal performance of microgrids in the worst case of renewable energy resource outage, which is in the upper-level problem of minimizing energy loss, and load shedding. It was formulated in the demand-side management program and modeled in the lower-level problem of maximizing output and reducing renewable energy resources. At the lower level, the worst-case realization of renewables is achieved, and at the upper level, the optimal operation of the distribution network is realized at the worst-case realization of renewable resources. A reformulation and decomposition based method considered to solve the proposed bi-level model, which is more reliable than similar method. The 33-node microgrid has been considered for the analysis of the proposed model and method, which proved the accuracy and optimal performance of the proposed model and method. In short, the following results were obtained after simulating different modes of renewable energy resources outage; a) the proposed model provides optimal operation by considering the worst-case renewable resource outage, which leads to reduced system vulnerability (load curtailment); b) considering that the proposed model is a mathematical optimization model of MIQP type, therefore, global optimal solutions are guaranteed by the Gurobi solver; c) due to the short time of solving the problem, it can be used for larger and online networks. To continue this study, the following are also recommended; 1) considering a multi-level model to investigate the impact of the outage of renewable energy resources at the level of the multi-area microgrids; b) considering the gas network and modeling power-to-gas (P2G) systems to investigate the conversion of surplus energy to gas and sale to the natural gas network.

ACKNOWLEDGMENT

The authors would like to thank Ghanai, Dr. Alibeaki, and Dr. Davarzani, who participated at the beginning of the work of the article, are greatly appreciated.

REFERENCES

[1] W. Yuan, Y. Wang, and Z. Chen, "New perspectives on power control of AC microgrid considering operation cost and efficiency," *IEEE Trans. Power Syst.*, vol. 36, no. 5, pp. 4844–4847, Sep. 2021, doi: 10.1109/TPWRS.2021.3080141.

[2] Z. Fan, B. Fan, J. Peng, and W. Liu, "Operation loss minimization targeted distributed optimal control of DC microgrids," *IEEE Syst. J.*, vol. 15, no. 4, pp. 5186–5196, Dec. 2021, doi: 10.1109/JSYST.2020.3035059.

[3] F. S. Al-Ismail, "DC microgrid planning, operation, and control: A comprehensive review," *IEEE Access*, vol. 9, pp. 36154–36172, 2021, doi: 10.1109/ACCESS.2021.3062840.

[4] Y. Jia, P. Wen, Y. Yan, and L. Huo, "Joint operation and transaction mode of rural multi microgrid and distribution network," *IEEE Access*, vol. 9, pp. 14409–14421, 2021, doi: 10.1109/ACCESS.2021.3050793.

[5] T. Nguyen, T. Dao, T. Nguyen, and T. Nguyen, "An optimal microgrid operations planning using improved archimedes optimization algorithm," *IEEE Access*, vol. 10, pp. 67940–67957, 2022, doi: 10.1109/ACCESS.2022.3185737.

[6] C. Wang, A. Wang, S. Chen, G. Zhang, and B. Zhu, "Optimal operation of microgrids based on a radial basis function meta-model," *IEEE Syst. J.*, vol. 16, no. 3, pp. 4756–4767, Sep. 2022, doi: 10.1109/JSYST.2021.3130760.

[7] Z. Li, L. Wu, Y. Xu, S. Moazeni, and Z. Tang, "Multi-stage real-time operation of a multi-energy microgrid with electrical and thermal energy storage assets: A data-driven MPC-ADP approach," *IEEE Trans. Smart Grid*, vol. 13, no. 1, pp. 213–226, Jan. 2022, doi: 10.1109/TSG.2021.3119972.

[8] F. Fallahi, M. Yildirim, J. Lin, and C. Wang, "Predictive multi-microgrid generation maintenance: Formulation and impact on operations & resilience," *IEEE Trans. Power Syst.*, vol. 36, no. 6, pp. 4979–4991, Nov. 2021, doi: 10.1109/TPWRS.2021.3066462.

[9] M. Chamana, K. E. K. Schmitt, R. Bhatta, S. Liyanage, I. Osman, M. Murshed, S. Bayne, and J. MacFie, "Buildings participation in resilience enhancement of community microgrids: Synergy between microgrid and building management systems," *IEEE Access*, vol. 10, pp. 100922–100938, 2022, doi: 10.1109/ACCESS.2022.3207772.

[10] H. Karimianfard and H. Haghighat, "Generic resource allocation in distribution grid," *IEEE Trans. Power Syst.*, vol. 34, no. 1, pp. 810–813, Jan. 2019, doi: 10.1109/TPWRS.2018.2867170.

[11] Z. Zhang, Z. Wang, H. Wang, H. Zhang, W. Yang, and R. Cao, "Research on bi-level optimized operation strategy of microgrid cluster based on IABC algorithm," *IEEE Access*, vol. 9, pp. 15520–15529, 2021, doi: 10.1109/ACCESS.2021.3053122.

[12] C. Wang, H. Yu, L. Chai, H. Liu, and B. Zhu, "Emergency load shedding strategy for microgrids based on dueling deep Q-learning," *IEEE Access*, vol. 9, pp. 19707–19715, 2021, doi: 10.1109/ACCESS.2021.3055401.

[13] J. Lee, S. Lee, and K. Lee, "Multistage stochastic optimization for microgrid operation under islanding uncertainty," *IEEE Trans. Smart Grid*, vol. 12, no. 1, pp. 56–66, Jan. 2021, doi: 10.1109/TSG.2020.3012158.

[14] Z. Zhao, J. Guo, X. Luo, C. S. Lai, P. Yang, L. L. Lai, P. Li, J. M. Guerrero, and M. Shahidehpour, "Distributed robust model predictive control-based energy management strategy for islanded multi-microgrids considering uncertainty," *IEEE Trans. Smart Grid*, vol. 13, no. 3, pp. 2107–2120, May 2022, doi: 10.1109/TSG.2022.3147370.

[15] S. Harasis, Y. Sozer, and M. Elbuluk, "Reliable islanded microgrid operation using dynamic optimal power management," *IEEE Trans. Ind. Appl.*, vol. 57, no. 2, pp. 1755–1766, Mar. 2021, doi: 10.1109/TIA.2020.3047587.

[16] N. Salehi, H. Martínez-García, G. Velasco-Quesada, and J. M. Guerrero, "A comprehensive review of control strategies and optimization methods for individual and community microgrids," *IEEE Access*, vol. 10, pp. 15935–15955, 2022, doi: 10.1109/ACCESS.2022.3142810.

[17] H. Karimianfard, M. R. Salehizadeh, and P. Siano, "Economic profit enhancement of a demand response aggregator through investment of large-scale energy storage systems," *CSEE J. Power Energy Syst.*, vol. 8, no. 5, pp. 1468–1476, Sep. 2022, doi: 10.17775/CSEEJPES.2021.02650.

[18] Y. Vilaisarn, Y. R. Rodrigues, M. M. A. Abdelaziz, and J. Cros, "A deep learning based multiobjective optimization for the planning of resilience oriented microgrids in active distribution system," *IEEE Access*, vol. 10, pp. 84330–84364, 2022, doi: 10.1109/ACCESS.2022.3197194.

[19] C. Reiz and J. B. Leite, "Optimal coordination of protection devices in distribution networks with distributed energy resources and microgrids," *IEEE Access*, vol. 10, pp. 99584–99594, 2022, doi: 10.1109/ACCESS.2022.3203713.

[20] Y. Vilaisarn, M. Moradzadeh, M. Abdelaziz, and J. Cros, "An MILP formulation for the optimum operation of AC microgrids with hierarchical control," *Int. J. Electr. Power Energy Syst.*, vol. 137, May 2022, Art. no. 107674.

[21] A. Singh and H. D. Nguyen, "A two-layer framework for optimal control of battery temperature and microgrid operation," *J. Energy Storage*, vol. 50, Jun. 2022, Art. no. 104057.

[22] M. Mansourlakouraj, M. Shahabi, M. Shafie-Khah, and J. P. S. Catalão, "Optimal market-based operation of microgrid with the integration of wind turbines, energy storage system and demand response resources," *Energy*, vol. 239, Jan. 2022, Art. no. 122156.

[23] H. Akulker and E. Aydin, "Optimal design and operation of a multi-energy microgrid using mixed-integer nonlinear programming: Impact of carbon cap and trade system and taxing on equipment selections," *Appl. Energy*, vol. 330, Jan. 2023, Art. no. 120313.

[24] E. Shokouhmand and A. Ghasemi, "Stochastic optimal scheduling of electric vehicles charge/discharge modes of operation with the aim of microgrid flexibility and efficiency enhancement," *Sustain. Energy, Grids Netw.*, vol. 32, Dec. 2022, Art. no. 100929.

[25] V. Bui, A. Hussain, and H. Kim, "A multiagent-based hierarchical energy management strategy for multi-microgrids considering adjustable power and demand response," *IEEE Trans. Smart Grid*, vol. 9, no. 2, pp. 1323–1333, Mar. 2018, doi: 10.1109/TSG.2016.2585671.

[26] K. Fabrice, C. Damour, D. Grondin, M. Hilairet, and M. Benne, "Multistage power and energy management strategy for hybrid microgrid with photovoltaic production and hydrogen storage," *Appl. Energy*, vol. 323, Oct. 2022, Art. no. 119549.

[27] S. M. Hosseini, R. Carli, and M. Dotoli, "Robust optimal energy management of a residential microgrid under uncertainties on demand and renewable power generation," *IEEE Trans. Autom. Sci. Eng.*, vol. 18, no. 2, pp. 618–637, Apr. 2021, doi: 10.1109/TASE.2020.2986269.

[28] S. S. Kheradmand, R. Haghpanah, M. B. Yazdi, and M. M. Farsangi, "Two mixed logical dynamical real-time receding horizon control schemes for microgrids operation optimization," in *Proc. 29th Iranian Conf. Electr. Eng. (ICEE)*, May 2021, pp. 302–306, doi: 10.1109/ICEE52715.2021.9544252.

[29] V.-H. Bui, A. Hussain, Y.-H. Im, and H.-M. Kim, "An internal trading strategy for optimal energy management of combined cooling, heat and power in building microgrids," *Appl. Energy*, vol. 239, pp. 536–548, Apr. 2019.

[30] M. Mehrasa, A. Sheikholeslami, M. Rezanejad, and J. Alipoor, "Inertia augmentation-based optimal control strategy of a weak grid-connected microgrid with PV unit and energy storage system," *J. Energy Storage*, vol. 62, Jun. 2023, Art. no. 106874.

[31] T. Hai, A. K. Alazzawi, J. Zhou, and T. Muranaka, "Optimal energy scheduling of microgrid with electric vehicles based on electricity market price," *J. Energy Resour. Technol.*, vol. 145, no. 6, Jun. 2023, Art. no. 061301, doi: 10.1115/1.4056526.

[32] O. Khoubseresht, M. Rajabinezhad, and S. Y. M. Mousavi, "An analytical optimum method for simultaneous integration of PV, wind turbine and BESS to maximize technical benefits," *IET Gener., Transmiss. Distrib.*, vol. 17, no. 10, pp. 2207–2227, 2023, doi: 10.1049/gtd2.12801.

[33] M. Pan, Q. Xing, Z. Chai, H. Zhao, Q. Sun, and D. Duan, "Real-time digital twin machine learning-based cost minimization model for renewable-based microgrids considering uncertainty," *Sol. Energy*, vol. 250, pp. 355–367, Jan. 2023.

[34] B. Zeng and Y. An, "Solving bilevel mixed integer program by reformulations and decomposition," Optimization Online, Univ. South Florida, Tampa, FL, USA, Tech. Rep., pp. 1–34, Jun. 2014.

[35] B. Zeng and L. Zhao, "Solving two-stage robust optimization problems using a column-and-constraint generation method," *Oper. Res. Lett.*, vol. 41, no. 5, pp. 457–461, Sep. 2013.

SAEID SHAKERINIA received the master's degree from Islamic Azad University, Shahroord Branch, in 2015, where he is currently pursuing the Ph.D. degree in electrical engineering.

ABBAS FATTAHI MEYABADI received the master's degree from Khaje Nasir University, Tehran, Iran, in 2005, and the Ph.D. degree in electrical engineering from the K. N. Toosi University of Technology, Tehran, in 2016. Since 2005, he has been a Faculty Member with the Hamedan University of Technology, Hamedan, Iran. His research interests include power system planning and electric vehicles.

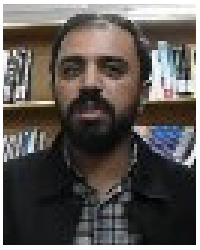

MOJTABA VAHEDI received the Ph.D. degree in electrical engineering from the Shahrood University of Technology, with a focus on control, in 2015. He have several articles in the field of electrical engineering. He also have supervised various students with Shahrood Azad University.

NASRIN SALEHI has been a Faculty Member with Islamic Azad University, Shahrood Branch, since 2005.

MAHMOUD SAMIEI MOGHADDAM received the master's degree from Khaje Nasir University, Tehran, Iran, in 2005, and the Ph.D. degree in electrical engineering from the K. N. Toosi University of Technology, Tehran, in 2016. Since 2005, he has been a Faculty Member with Islamic Azad University, Damghan Branch, Damghan, Iran. His research interests include power system planning and electric vehicles.